International Journal of Steel Structures (2018) 18(5):1577–1588
https://doi.org/10.1007/s13296-018-0054-6

Online ISSN 2093-6311
Print ISSN 1598-2351

Experimental Study and Confinement Analysis on RC Stub Columns Strengthened with Circular CFST Under Axial Load

Hongjun Liang[1,2] · Yiyan Lu[2] · Jiyue Hu[2] · Jifeng Xue[2]

Received: 30 April 2017 / Accepted: 19 March 2018 / Published online: 26 April 2018

Abstract

As the excellent mechanical performance and easy construction of concrete filled steel tubes (CFST) composite structure, it has the potential to be used to strengthen RC pier columns. Therefore, tests were conducted on 2 reinforcement concrete (RC) stub columns and 9 RC columns strengthened with circular CFST under axial loading. The test results show that the circular CFST strengthening method is effective since the mean bearing capacity of the RC columns is increased at least 3.69 times and the ductility index is significantly improved more than 30%. One of the reasons for enhancement is obvious confinement provided by steel tube besides the additional bearing capacity supplied by the strengthening materials. From the analysis of the enhancement ratio, the strengthening structure has at least an extra 20% amplification except for taking full advantage of the strength of the strengthening material. Through the analysis of confining stress provided by steel tube and the stress–strain relationship of confined concrete, it is found that the strength of the core concrete can be increased by 21–33% and the ultimate strain can be enhanced to beyond 15,000 $\mu\varepsilon$.

Keywords RC columns · Circular CFST · Strengthening method · Axial loading

1 Introduction

The annual worldwide investment on corrosion related maintenance and repair of RC structures totals \$100 billion (Li and Melchers 2005). One of the main reasons is aging of the infrastructure. Some of the structures are damaged by environmental effects which include corrosion of steel, freeze—thaw cycles and concrete carbonation. These effects result to rebar corrosion and concrete cracking, thereby structural deterioration. On the other hand, many structures need to be strengthened because of the increasing allowable loads, new functional requirements and new super standard codes. How to repair and strengthen these deficient structures is a tremendous issue which needs to pay more attention.

Most common methods for repair and retrofit of RC columns are concrete jacketing (Vandoros and Dritsos 2008; Julio and Branco 2008), steel jacketing (Adam et al. 2007; Xiao and Wu 2003; Abedi et al. 2010; Aboutaha et al. 1999a, b; Aboutaha and Machado 1999) and FRP wrapping (Hadi 2007; Colomb et al. 2008; Dai et al. 2011; Parvin and Wang 2002; Lu et al. 2007). In this paper, CFCST composite structure is used to strengthen deficient RC columns, which is a combined variation of the steel jacketing and concrete jacketing. The strengthening procedure consisted of striping off the protective layer and deteriorated concrete of the deficient RC columns, packing a circular steel tube jacket welded by two pieces of semicircular steel plates and casting self-compacting concrete in the gap to make the RC columns and the steel tube become an integral. The strengthening method is recognized as being easy to construct. Meanwhile, the construction time and cost will be reduced compared with concrete jacketing, because the steel tube can serve as a shuttering and steel cage. It also needs less welding than the steel jacketing strengthening method. Moreover, it was showed from the results of a great deal of research on CFST (Gupta et al. 2007; Han and Yao 2004; Lu et al. 2007; Sakino et al. 2004; Uy et al. 2011) that the strength and the ductility of the RC concrete and strengthening concrete are enhanced due to the additional confinement given by the exterior steel tube, while the concrete core can also delay the steel tube

✉ Yiyan Lu
yylu901@163.com

1 School of Civil Engineering and Mechanics, Huazhong University of Science and Technology, Wuhan 430072, Hubei Province, China

2 School of Civil Engineering, Wuhan University, Wuhan 430072, Hubei Province, China

from local buckling (Elremaily and Azizinamini 2002).The characteristics of easy construction, relatively inexpensive and excellent mechanics performance urge CFCST composite structure to have the potential to strengthen RC columns.

Continuous research efforts related to the CFST strengthening method have been conducted. Priestley et al. (1994a, b) performed experimental and theoretical investigation to determine the enhanced shear strength of RC columns strengthened with elliptical CFST. The results indicated that the lateral stiffness of the strengthening columns was increased by an average of 64% and the ductility was significantly improved. Miller (2006) and Sezen and Miller (2011) carried out experimental comparisons about the behavior of 15 circular RC columns strengthened with FRP wraps, circular CFST or concrete jackets under axial load. The comparative results show that the circular CFST strengthening method is more effective to improve the specimen stiffness, member strength and ductility because of the existence of sufficient confinement. Wang (2011) studied the behavior of the RC columns with- and without initial stress conditions strengthened with circular CFST under axial load. It was reported that the initial stress had less influence on the ultimate bearing capacity of the strengthened columns while had some adverse impact on the ductility. The main reason is that the effective strengthening enhancement on the bearing capacity and ductility will weaken the influence of initial stress so that less and less research focused on initial stress conditions. Zhou et al. (2012) conducted axial loading tests on 6 circular RC columns strengthened with circular CFST. They reported that the constraint function of steel tube on the internal concrete is obvious and the confinement effect becomes more obvious with the increase of wall thickness. Lu et al. (2015a, b) carried out experimental comparisons of the capacity of RC columns strengthened with square and circular CFST. The results indicated that the circular tube could provide more effective confinement than the square tube, while the square tube possessed more convenient construction and simpler node structure.

However, the use of this strengthening method has been limited in practical project due to a lack of adequate experimental data about the strength and in-depth explanation of the confining mechanism in the circular CFST strengthening system. Therefore, the primary objective of this paper is to present an experiment to investigate the enhancement performance of strengthened columns include failure mode, bearing capacity, axial stiffness and ductility. Furthermore, a quantitative analysis of confining stress provided by steel tube is obtained and analyzed. The enhancement of core concrete is also investigated due to the confining stress.

2 Experimental Program

2.1 Test Specimens Details

The experiment involved construction, strengthening and testing of 11 stub column specimens. Two bare columns, named RC1 and RC2, were tested as a reference or control specimen without any strengthening. The bare specimens had a clear height of 800 mm with a cross-section of 150 mm by 150 mm as shown in Fig. 1a. The remaining 9 RC columns were strengthened with circular CFST. According to

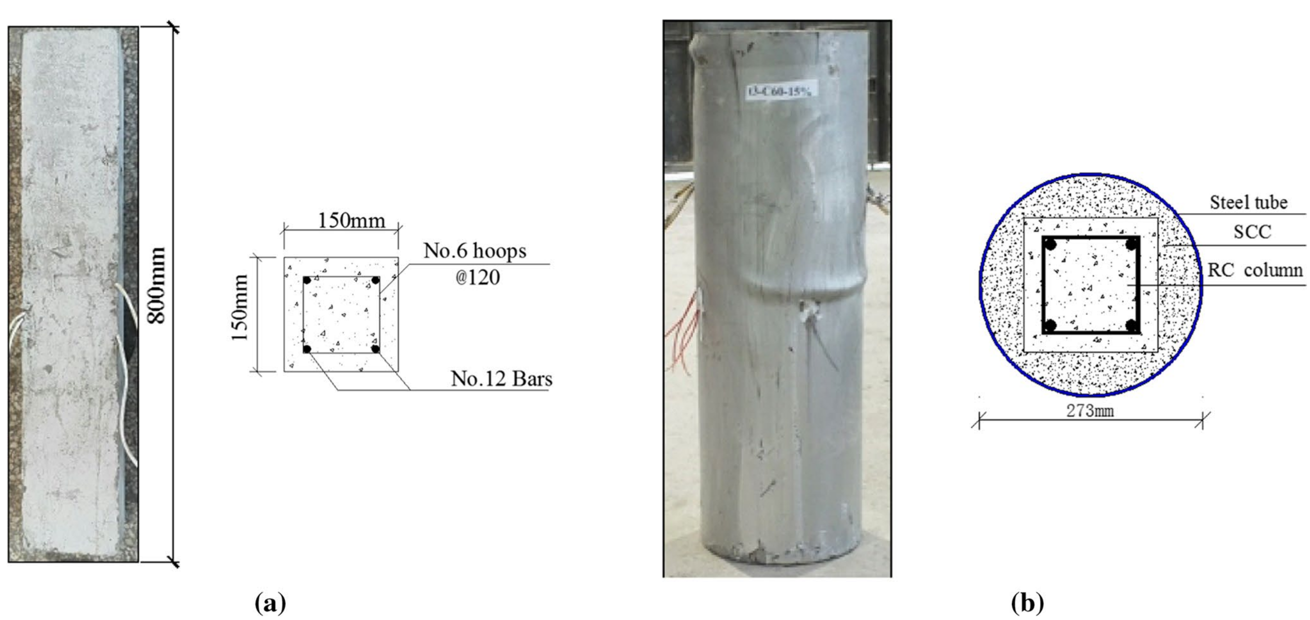

Fig. 1 Geometrical size of specimens. **a** RC column, **b** SRC column

the requirements of China's strengthening standard, the narrowest gap between RC column and steel tube requires more than twice the maximum particle size of coarse aggregate. Therefore, the cross-section of the strengthened column was designed as 273 mm, the narrowest gap was 31 mm, and the maximum particle size of coarse aggregate was less than 15 mm. Meanwhile, in order to ensure the safety of the strengthening structures in the earthquake, the general design requirement is required to meet "strong column, weak beam, and stronger joints". Therefore, strengthening column-beam joint need to be reinforced through welded angle steel and plug bolt in the practical CFST strengthening project. Inevitably the steel will directly contribute to the load bearing capacity besides provide confinement. In order to simulate the real load condition, the height of steel tube was set to the same as the RC column to ensure the axial load simultaneously applied on the steel tubes and the concrete core. The cross section details are shown in Fig. 1b. All the details are summarized in Table 1. The nomenclature of strengthened columns followed in the tests is: SRCX-CY (i.e. SRC3-C40), where X represents for the design tube thickness, and Y is the design concrete grade.

2.2 Material Properties

2.2.1 Concrete

As model columns simulating deficient columns, the RC columns were poured with normal pre-mix concrete whose design strength was low to 30 MPa. Because of the narrow gap between the RC columns and steel jacket, self-compacting concrete (SCC) was cast, which allows pouring concrete easily without vibration even in the presence of a highly dense rebar or novel form of construction (Muciaccia et al. 2011; Holschemacher 2004). The concrete mixtures were made with Portland cement, river sand, granite stone of particle size 5–15 mm, fly ash and silica fume. Super-plasticizer was used to ensure a workability of self-consolidating. Slump flow of the SCC was beyond 650 mm which meets casting requirement as shown in Fig. 2. The design strength grade of the strengthening concrete varies between C35, C45 and C55. The cube concrete compressive strength 'f_{cu}' is determined by testing the cube specimens of dimensions $150 \times 150 \times 150$ mm after 28 days of curing. The mean measured cube strengths for the C30, C35, C45 and C55 concrete were 31.52, 36.63, 44.87 and 54.69 MPa, respectively.

2.2.2 Steel

The RC columns were reinforced with four 12 mm diameter longitudinal bars and were transversely reinforced with 6 mm diameter hoops, spaced at 120 mm. The clear concrete cover to the hoops was 20 mm. The average values of yield strength, ultimate tensile strength and elastic modulus for the longitudinal bars were 458, 615 MPa and 200 GPa, respectively. For SRC columns, three types of steel plates, with design thickness of 2, 3 and 4 mm, were used to fabricate the steel tubes and achieve different diameter-to-thickness ratios. Tensile tests on three steel coupons which were taken from the semicircular steel jacket and the steel rebar were conducted. The real measured thicknesses of three types of tubes are 2.10, 3.16 and 4.14 mm, respectively. The real diameter-to-thickness ratios varied from 66 to 130. The average values of yield strength, ultimate tensile strength and elastic modulus were 353, 445 MPa and 205 GPa, respectively.

Table 1 Geometrical and material parameters for all test specimens

Specimen	$D \times L$ (mm)	D/t	f_{cu1} (MPa)	f_{cu2} (MPa)	f_{y1} (MPa)	f_{y2} (MPa)	N_e (kN)
RC1	150×800	–	31.52	–	458	–	714
RC2	150×800	–	31.52	–	458	–	697
SRC2-C30	273×800	130	31.52	36.63	458	353	2608
SRC2-C40	273×800	130	31.52	44.87	458	353	2951
SRC2-C50	273×800	130	31.52	54.69	458	353	3219
SRC3-C30	273×800	86	31.52	36.63	458	353	2873
SRC3-C40	273×800	86	31.52	44.87	458	353	3252
SRC3-C50	273×800	86	31.52	54.69	458	353	3484
SRC4-C30	273×800	66	31.52	36.63	458	353	3143
SRC4-C40	273×800	66	31.52	44.87	458	353	3465
SRC4-C50	273×800	66	31.52	54.69	458	353	3845

D, L and t are real diameter, height and thickness of steel tube, respectively; f_{cu1} and f_{cu2} are the cube strengths of RC column concrete and strengthening concrete, respectively; f_{y1} and f_{y2} are the average values of yield strength of longitudinal bars and steel tube, respectively; N_e is the ultimate load obtained from experimental result

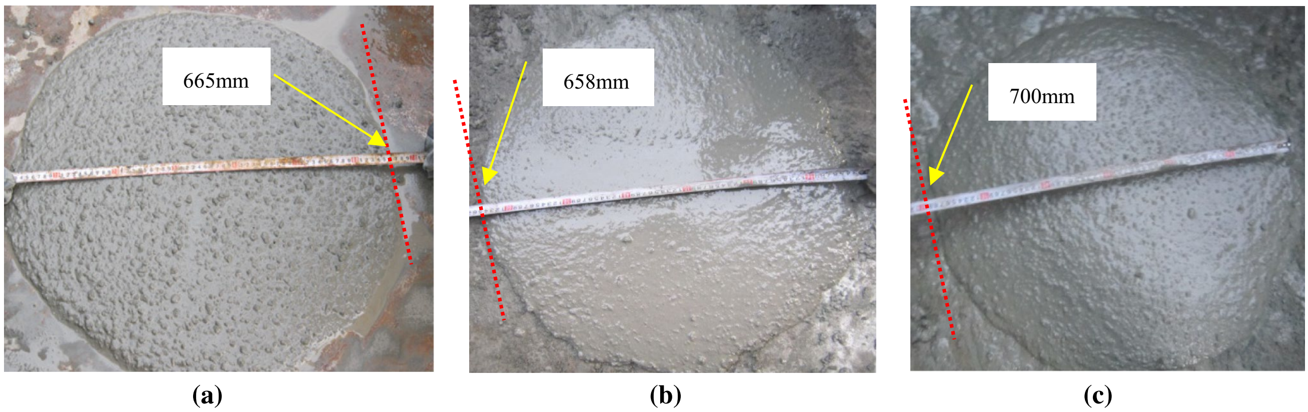

Fig. 2 Slump flow of SCC. **a** C35, **b** C45, **c** C55

2.3 Test Setup and Instrumentation Layout

All the tests were performed under a 5000 kN capacity universal testing machine. The test setup and instrument layout are shown in Fig. 3. The specimens were placed into the testing machine and two thick stiff plates were placed on the ends of the specimens to ensure the axial load applied simultaneously to the steel tubes and the concrete core. A force transducer was placed below the bottom to accurately measure the applied axial load in real-time. Two linear variable displacement transducers (LVDTs) were placed on both sides of the specimens to measure the axial shortening. Eight electrical strain gauges were glued to the external surface of the square steel tubes at mid-height to measure the axial and hoop strains in four locations 0°, 90°, 180° and 270°, and another four strain gauges were glued on the longitudinal rebar to measure the axial strains. A computerized data-acquisition system was used to collect the experimental data of the load, deformation and strain.

3 Experimental Results and Discussions

3.1 Failure Mode

Typical failure modes of RC and SRC columns are compared in Fig. 4. The RC columns failed suddenly by crushing of the concrete cover once reaching the peak load and serious buckling of the longitudinal rebar. It can be seen from Fig. 4a that several long and wide cracks appeared on concrete cover coincided with massive concrete spalling. The max axial shortening of WRC columns was about 6 mm. However for SRC columns as shown in Fig. 4b, the SRC specimens behaved in a relatively ductile manner. The applied load maintains at a certain loading level after the

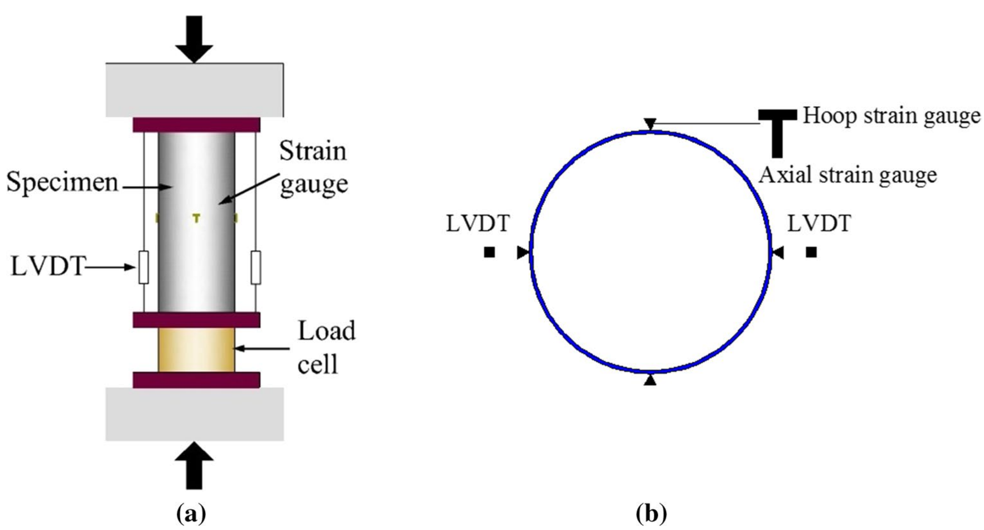

Fig. 3 Test setup and instrumentation. **a** Setup, **b** layout of measuring points

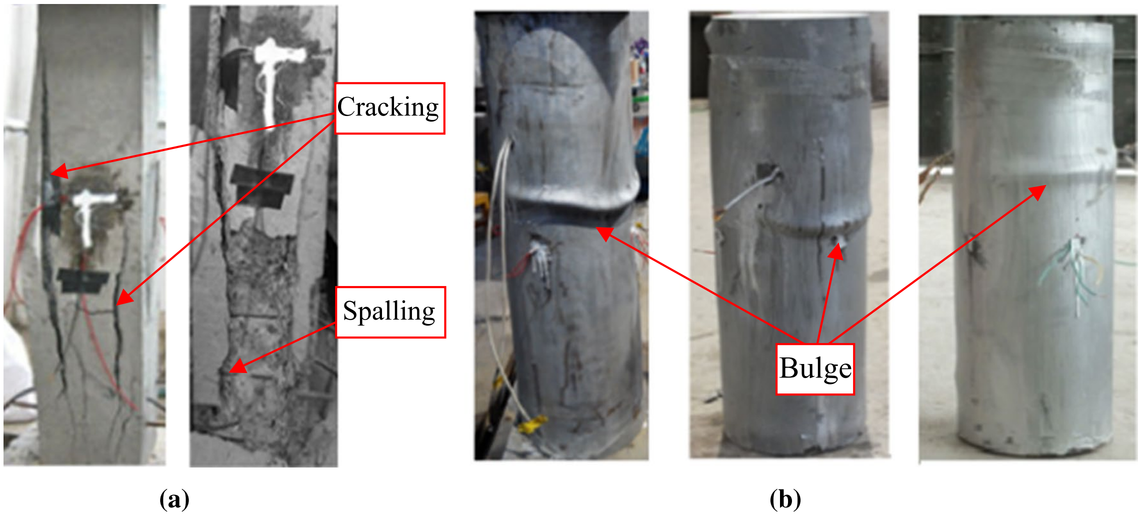

Fig. 4 Typical failure modes. **a** RC, **b** SRC

ultimate load, while the deformation is still aggravating. The specimens experienced outward local buckling of the steel tubes because of the stability supplied by the infill of SCC concrete. One obvious bulge was observed near the mid-height of specimens. The axial shortening of the SRC columns was obvious and even beyond 20 mm. These phenomena reveal that circular CFST strengthening method could increase the deformation capacity of the RC columns and make the failure mode become more ductile.

3.2 Axial Load-Shortening Behavior

Axial load N-axial shortening Δ curves of all the specimens are shown in Fig. 5, where Δ is an average value measured from LVDTs. These curves were grouped into three parts to illustrate influence of strengthening method (as shown in Fig. 5a), steel thickness (as shown in Fig. 5b) and concrete strength (as shown in Fig. 5c) on the axial stiffness, ultimate strength and ductility of specimens. The $N-\Delta$ curves can be approximately divided in three stages: the elastic stage, the elastic–plastic stage and the failure stage. In the early load, the $N-\Delta$ curves are close to linearity. To quantitatively analyse the axial stiffness of specimens, a stiffness index (*SI*) is defined as tangent stiffness and equal to the slope of curve fitting of the linear elastic stage. The fitting line is plotted by a dotted line in Fig. 5 and the values of SI are presented in Table 2. It is shown in Fig. 5a and Table 2 that the $N-\Delta$ curves of typical SRC column (SRC3-C40) exhibit greater slope and longer linear stage than that of RC columns and the SI of the SRC columns is 2.14–3.12 times of the RC columns.

Subsequently, the specimens reach the ultimate load through a short and smooth elastic–plastic stage. It is found that the ultimate loads of RC columns are significantly increased by circular CFST strengthening method. The ultimate strength of the strengthened columns is 3.65–5.39 times of the RC columns. Referring to the relevant literature about circular CFST composite columns (Tao et al. 2011; Han et al. 2009, 2011), obvious confinement provided by steel tube is one of the reasons for high carrying capacity. Therefore, another numerical index *EI* (enhancement index) defined in Han et al. (2014) was adopted here to quantify the enhancement in carrying capacity as:

$$ER = \frac{N_{\mathrm{e,SRC}}}{N_{\mathrm{e,RC}} + N_{\mathrm{c}}} \tag{1}$$

$$N_c = 0.85A_{c2}f'_{c2} + A_{s2}f_{y2} \tag{2}$$

where, $N_{\mathrm{e,SRC}}$ and $N_{\mathrm{e,RC}}$ are the measured ultimate load of SRC strengthened specimens and RC original specimens; A_{c1} and A_{s2} are the cross-sectional areas of the strengthening concrete and the steel tube, respectively; f'_{c2} and f_{y2} are the compressive strengths of the strengthening concrete and the yield strength of steel tube. The values of ER are listed in Table 2. The average of *CR* for the test stub specimens is 1.20, which means this composite structure has at least an extra 20% amplification except for taking full advantage of the strength of material and RC columns. The data denote that the steel tubes can provide an efficiently confinement to the concrete core in the SRC columns.

After ultimate load, the $N-\Delta$ curves begin to slide, but the SRC group behaves a more gentle descent stage. The *DI* (ductility index) proposed in Han et al. (2014) is introduced here according to the $N-\Delta$ curves to quantify the ductility as:

$$DI = \frac{\Delta_{0.85}\mathrm{max}}{\Delta_{\mathrm{max}}} \tag{3}$$

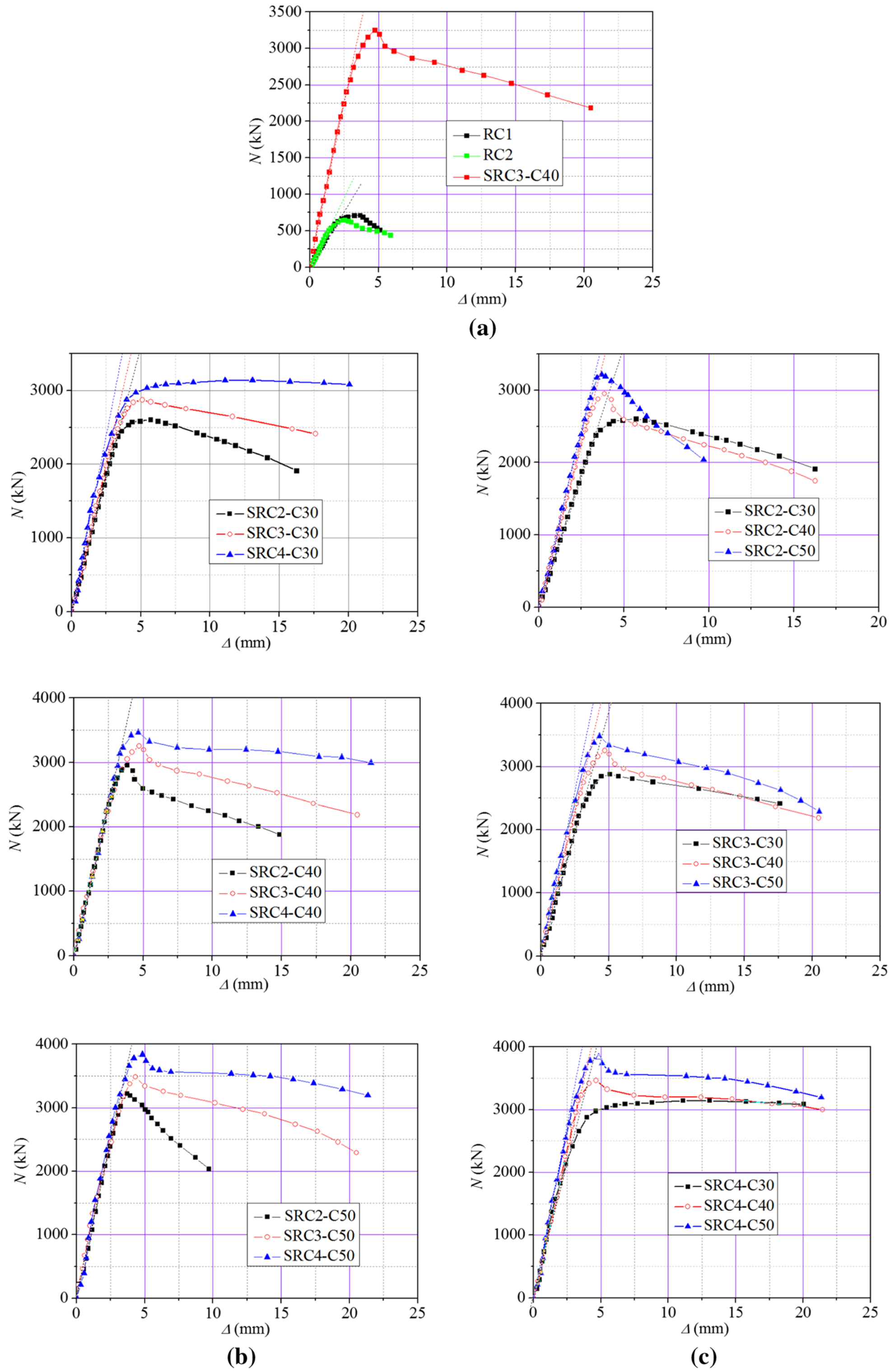

Fig. 5 Axial load *N*-axial shortening *Δ* curves. **a** RC and typical SRC columns, **b** SRC columns with different tube thickness, **c** SRC columns with different concrete strength

in which, $\Delta_{0.85\max}$ is the axial shortening when the load falls to 85% of the ultimate load (in the descending branch) and the $\Delta_{\max}$ is the axial shortening corresponding to the ultimate load. Table 2 reveals that the *DI* of SRC column is at least 30.50% more than that of RC column. The data imply the axial stiffness and ductility of the RC columns have been significantly improved by circular CFST.

As shown in Fig. 5b, the $N-\Delta$ curves of SRC with different diameter-to-thickness ratios (except C30 series) have approximate equivalent slopes. It could be found in Table 2

Table 2 Performance indices for all test specimens

Specimen	*D/t*	f_{cu2} (MPa)	*SI*	*ER*	*DI*
RC1	–	–	337	–	1.14
RC2	–	–	354	–	1.22
SRC2-C30	130	36.63	739	1.18	2.16
SRC2-C40	130	44.87	889	1.22	1.61
SRC2-C50	130	54.69	969	1.22	1.54
SRC3-C30	86	36.63	762	1.16	3.31
SRC3-C40	86	44.87	898	1.22	2.90
SRC3-C50	86	54.69	1012	1.21	2.12
SRC4-C30	66	36.63	904	1.16	+ ∞
SRC4-C40	66	44.87	940	1.20	+ ∞
SRC4-C50	66	54.69	1043	1.24	+ ∞

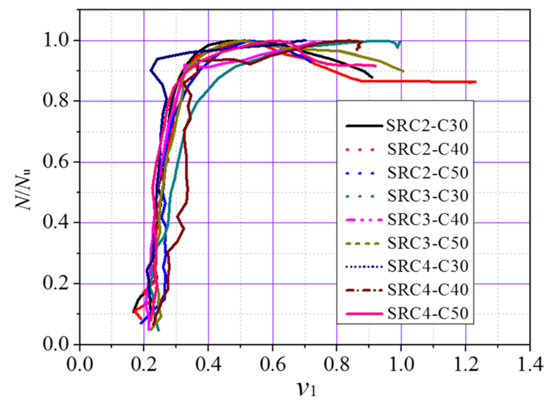

Fig. 6 Relative load versus dilation ratio curves

that the maximum disparity of *DI* between SRC-C40 series is only 5.78%, and that for SRC-C50 series is 4.25% so that the linear stages of curves in Fig. 5b are fitted by a same line. However for SRC-C30 series, the maximum disparity is increased to 15.69%. It is mainly due to the greater modulus of elasticity (E_c) of higher strength concrete decrease the proportion of steel tube in axial stiffness of composite structure so that the influence generated by the difference in steel thickness is weakened. And then, the descent stage tends gentler when increasing the steel thickness. It was surprisingly found in Table 2 that the SRC4 series have infinite *DI* because the load is decreased no less than 0.85 N_u until loading end.

It is also apparent that in Fig. 5c, the $N-\Delta$ curve of SRC with C50 concrete possesses greater slope. The SI of SRC2-C50 shown in Table is 23.74 and 8.26% more than that of SRC2-C40 and SRC2-C30, respectively. However, the SRC with C50 behave poorer ductility than others. The *DI* of SRC2-C50 is 40.26% less than that of SRC2-C30, and the DI of SRC3-C50 is 56.1% less than that of SRC3-C30. Thus many design codes such as Eurocode4 limit the use of high strength (more than 60 MPa) concrete to guarantee a good ductile behavior of the concrete filled steel tube columns. However, the ductile behavior is still achieved if the steel tube is thick enough (i.e. SRC4-C50) due to the strong confinement.

3.3 Relative Load-Dilation Ratio

In order to reflect the confinement during the loading, the relative load (N/N_u) versus dilation ratio (v_1) curves of the strengthened columns are presented in Fig. 6. The v_1 is defined as the ratio of the hoop strain and axial strain of strengthened column measured by the strain gauges. It is found that the v_1 of the strengthened columns range from 0.2 to 0.25 which is close to the Poisson's ratio of steel, and higher than that of concrete (about 0.17–0.20) before the applied load is up to approximately 80% of the ultimate load. It means the lateral expansion of steel tube is larger than that of concrete under the same axial shortening at this stage. Therefore the steel tubes have no confining effect on the concrete core. Subsequently, the v_1 increases rapidly even beyond 1.0 which is significantly larger than that of steel as the applied load increases. It is considered to be caused by the expansion of concrete. At this stage, a radial stress develops at the steel–concrete interface, which subjects the concrete core to tri-axial stress, thereby enhancing the concrete strength. The confining effect will continue to work until the end of loading. Related quantitative analysis of the confinement will be presented in the following section.

3.4 Confining Stress Provided by Steel Tube

In order to quantitatively analyze the confinement, confining stress state of steel tube is needed to be determined. In a SRC strengthened column, the steel tube is subjected to axial stress (σ_z), circumferential tensile stress (σ_θ), and radial stress (σ_r), or in other words, under triaxial stress state as shown in Fig. 7. The σ_θ and σ_r may be evaluated from the following equilibrium conditions:

$$\sigma_r = -\frac{2t}{D-2t}\sigma_\theta = -\frac{2}{(t/D)-2}\sigma_\theta \tag{4}$$

In this research, the thickness of thin-walled steel tube is very small compared to the diameter so that the magnitude of radio stress is negligible compared to the circumferential stress. The ratio of σ_r and σ_θ varied from 1.6 to 3.1% in this analysis. Hence, the steel tube may be assumed to be subjected to axial loading and circumferential tension only, or in other words, under a state of plane stress. The stresses of the mid-height section of the tube during the loading process can be determined from the two measured strains (i.e., the axial strain and the circumferential strain) based on the

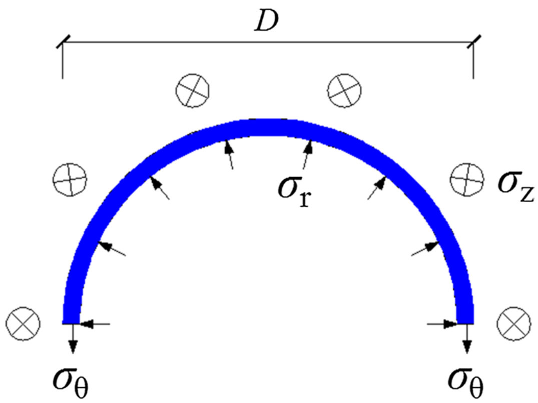

Fig. 7 Confining stress state of the steel tube

stress–strain relations. In present study, the steel is simply assumed to be an elastic-perfectly plastic material (Chen and Saleeb 1982). The analysis basically involves the calculation of stress increments from strain increments by using the following two equations [Eq. (5) for the elastic stage and Eq. (6) for the elastic–plastic stage]:

$$\begin{bmatrix} d\sigma_z^i \\ d\sigma_\theta^i \end{bmatrix} = \frac{E_s}{1-\nu^2}\begin{bmatrix} 1 & \nu \\ \nu & 1 \end{bmatrix}\begin{bmatrix} d\varepsilon_z^i \\ d\varepsilon_\theta^i \end{bmatrix} \quad (0 \le \bar{\sigma} \le f_p) \tag{5}$$

$$\begin{bmatrix} d\sigma_z^i \\ d\sigma_\theta^i \end{bmatrix} = \frac{E_s}{1-\nu^2}\begin{bmatrix} 1-\left(S_a^2/S_c\right) & \nu-\left(S_aS_b/S_c\right) \\ \nu-\left(S_aS_b/S_c\right) & 1-\left(S_b^2/S_c\right) \end{bmatrix}\begin{bmatrix} d\varepsilon_z^i \\ d\varepsilon_\theta^i \end{bmatrix} \quad (f_p \le \bar{\sigma} < f_y) \tag{6}$$

where

$$s_a = s_z + \nu s_\theta \tag{7}$$

$$s_b = s_\theta + \nu s_z \tag{8}$$

$$s_c = s_z^2 + s_\theta^2 + 2\nu s_\theta s_z \tag{9}$$

$$s_x = \frac{1}{3}\left(2\sigma_z^{i-1} - 2\sigma_\theta^{i-1}\right) \tag{10}$$

$$s_\theta = \frac{1}{3}\left(2\sigma_\theta^{i-1} - 2\sigma_z^{i-1}\right) \tag{11}$$

in which ε_x and ε_θ are axial and circumferential strains, respectively; E_s and ν are elastic modulus and Poisson's ratio of the steel, respectively; and i is the present strain increment number. The von Mises yield criterion is given by:

$$\left(\sigma_x^{i-1}\right)^2 + \left(\sigma_\theta^{i-1}\right)^2 + \sigma_x^{i-1}\sigma_\theta^{i-1} - f_{y2}^2 = 0 \tag{12}$$

where f_{y2} is yield stress of the steel tube. In Eqs. (5)–(12), tensile stresses and strains are defined to be negative, whereas compressive stresses and strains are positive. Referring to the relevant literatures (Kwan et al. 2016; Abed et al. 2013; Han et al. 2005), the Poisson's ratio of steel was approximately 0.3.

Figure 8 presents the radial stress (σ_r), which can also be called confining stress, calculated by Eq. (4) against the axial strain. As expected, the confining stress is approximate to or slight more than 0 because of no confining effect as previous discussion. When the axial strain is over 2000 $\mu\varepsilon$, the confining stress is seen to increase rapidly. After the axial strain is beyond 5000 $\mu\varepsilon$, the confining stress reaches the peak and is kept constant. Generally, the ultimate confining stress increases with the steel thickness increasing, while the strength of the strengthening concrete has relatively small influence. The biggest stress generated in SRC4-C30 is 2.2 MPa, while the least stress appeared in SRC2-C50 is 1.0 MPa.

3.5 Proposed Models for Confined Concrete

Due to the presence of confining stress, the expansion of the concrete core will be confined by the exterior steel tube. Consequently, the concrete core is subjected to triaxial stress, and thereby the strength is enhanced. To quantify the enhancement, many models were proposed based directly on the regression of test data or theoretical modes based on elastoplastic mechanics, which generally make use of some simple assumptions. The form of these models for the peak axial stress f_{cc} of the confined concrete can be expressed as the following equation:

$$f_{cc} = f_c' + k\sigma_r \tag{13}$$

in which k represents the coefficient of confining stress which is taken as different values in different models. In the model of Xiao et al. (2010), k was considered to be equal to $3.24\left(\sigma_r/f_c'\right)^{-0.2}$ (in the range of 5.27–6.67 in this paper), whereas k was taken as $-2.228\left(\sigma_r/f_c'\right) + 2.172\sqrt{\left(\sigma_r/f_c'\right)^2 + 7.46\left(\sigma_r/f_c'\right)} - 2$ (in the range of 3.66–4.45 in this paper) in the model of Abdalla et al. (2013), and approximately equal to $1.14\left(f_c'/\sigma_r\right)$ (in the range of 2.59–5.16 in this paper) in the model of Han et al. (2005).

In summary, the value k is generally believed to be between 3 and 6. The rough strength of confined concrete can be estimated by the above formula, but the accuracy need to be further developed. Therefore, this paper conducted

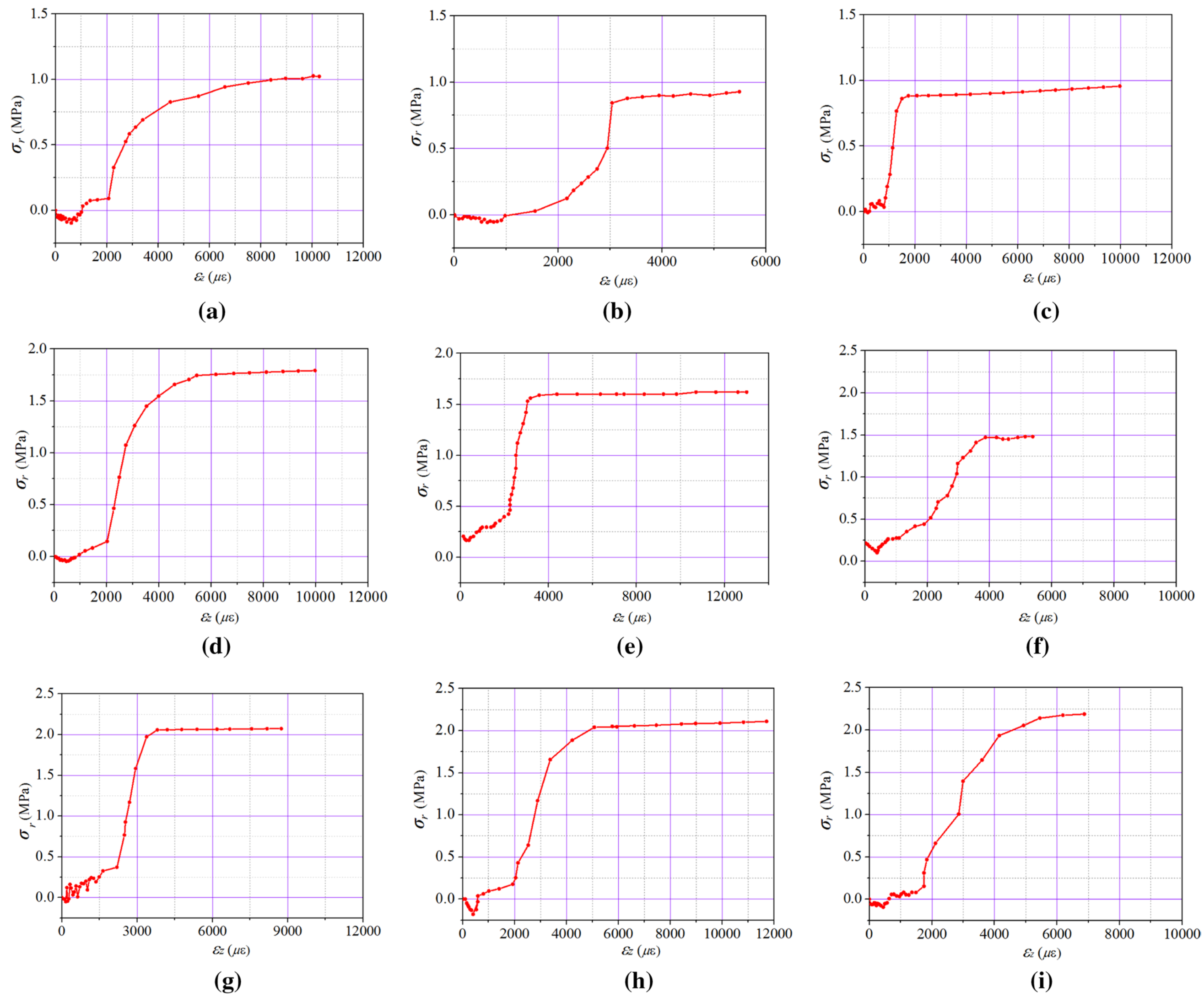

Fig. 8 Confining stress at the steel–concrete interface. **a** SRC2-C30, **b** SRC2-C40, **c** SRC2-C50, **d** SRC3-C30, **e** SRC3-C40, **f** SRC3-C50, **g** SRC4-C30, **h** SRC4-C40, **i** SRC4-C50

more in-depth analysis based on the test results to obtain actual strength of confined concrete and the complete axial stress–strain curves under different confining stresses.

3.6 The Stress–Strain Curves of Confined Concrete

In the case of determining the axial stress of the steel tube and the steel rebar, the axial load carried by the confined concrete can be found by deducting the axial loads carried by the steel tube and rebar from the total load acting on the specimen, thereby obtaining the axial stress of whole concrete. The axial strain can be considered as the ratio of axial shortening and clear height. Thus, the complete axial stress–strain curve will be obtained.

The longitudinal rebar is considered uniaxial compression. The axial load carried by the steel rebar occupies a very small percentage because of the small cross-sectional area so that it has little influence on the total load acting on the strengthened column. Therefore, the stress–strain relation for steel rebar is simplified to bilinear models as following form in the analysis,

$$\sigma_{s1} = \begin{cases} f_{y1} & (\varepsilon \geq \varepsilon_{y1} = f_{y1}/E) \\ \varepsilon E_1 & (-\varepsilon_{y1} \leq \varepsilon < \varepsilon_{y1}) \\ -f_{y1} & (\varepsilon < -\varepsilon_{y1}) \end{cases} \tag{14}$$

in which f_{y1}, E_1 and ε_{y1} are the yield stress, the elastic modulus and the yield strain of steel rebar, respectively.

The axial strains of core concrete and steel tube are assumed to be equal. The obtained axial stress-axial strain curves of confined concrete are then plotted in Fig. 9. In

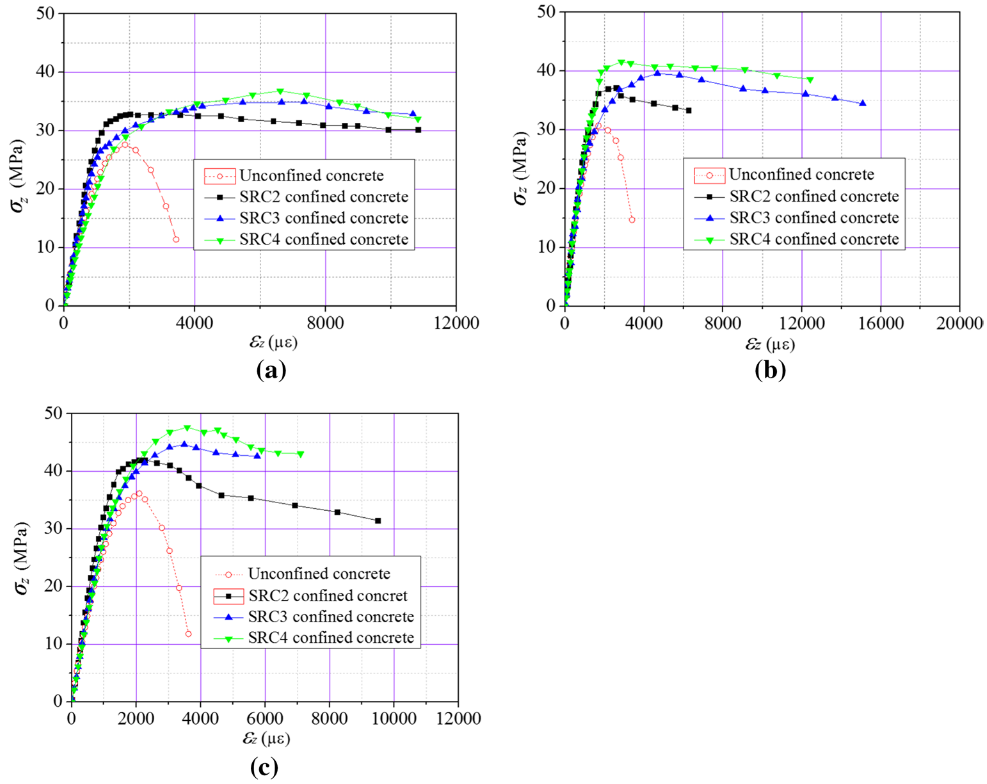

Fig. 9 The stress–strain curves of the confined concrete. **a** C30, **b** C40, **c** C50

order to analyze the enhancement of confined concrete, the stress–strain curves of unconfined concrete with same concrete equivalent strength calculated by models proposed in (Yalcin and Saatcioglu 2000) are compared in Fig. 9. In this paper, the RC column concrete and strengthening concrete were simplified to a whole. Meanwhile, the whole concrete is considered to a compatible deformation when the column deflects. Therefore, the equivalent strength of whole concrete can be calculated by Eq. (15).

$$f_c = (f_{c1}A_{c1} + f_{c2}A_{c2})/(A_{c1} + A_{c2}) \tag{15}$$

in which f_c is equivalent strength of whole concrete, A_{c1} and A_{c2} are the cross-sectional areas of the RC column and strengthening concrete, f_{c1} and f_{c2} are the cylinder compressive strengths of RC column concrete and strengthening concrete.

As expected, the curves of the un- and confined concrete have a similar slope due to no confining effect in the initial loading stage. Then it is obviously observed that the confined concrete, as expected, reaches higher peak stress than the unconfined concrete through a longer smooth curve. The peak stress of the curves are summarized in Table 3, it is evident that the peak stress of unconfined concrete can be significantly increased by 21–33%. Moreover, the coefficient k changed from 4.59 to 5.59 through the calculation in this research which fall in the range of 3–6.

Furthermore, for unconfined concrete, the curve features a rapid descending branch following the attainment of the peak stress at a relatively small axial strain. The ultimate strain of unconfined concrete is about 3500 $\mu\varepsilon$. By contrast, the confined concrete has a slowly descending branch and a larger ultimate strain. As some strain gauges are damaged before the end of loading, the curves of some specimens (i.e. SRC2-c40) are not complete. However, from the specimens SRC3-C40, it is obvious that the ultimate strain of confined concrete can even achieve nearly 15,000 $\mu\varepsilon$ which is approximately equal to 5 times of that of unconfined concrete.

Table 3 The peak stress of confined concrete

Specimens	f_c/MPa	f_c^u/MPa	k_1	k
SRC2-C30	27.68	32.68	1.18	5.00
SRC2-C40	31.66	36.87	1.16	5.21
SRC2-C50	36.40	41.6	1.14	5.20
SRC3-C30	27.66	34.96	1.26	4.87
SRC3-C40	31.59	39.28	1.24	5.13
SRC3-C50	36.28	44.67	1.23	5.59
SRC4-C30	27.63	36.82	1.33	4.59
SRC4-C40	31.53	41.59	1.32	5.03
SRC4-C50	36.17	46.79	1.29	5.31

f_c^u is the peak stress of confined concrete, $k_1 = f_c^u/f_c$, k is the coefficient of confining stress

4 Conclusion

This paper presented an experimental study to gain a better understanding of the behavior of RC stub columns strengthened with circular CFST under axial loading. The influence of steel tube thickness (2–4 mm) and strengthening concrete strength (C30–C50) on the enhanced performance of the strengthened columns were investigated. The results reached within the scope of the study showed that the circular CFST strengthening method is highly effective since bearing capacity, stiffness and deformation capacity of the RC columns are improved significantly. The bearing capacity of RC columns are increased at least 3.69 times and the ductility index (*DI*) are improved more than 30%. The confinement provided by steel tube is one of the main reasons to increase the performance of strengthened columns, which can cause at least an extra 20% amplification except for taking full advantage of the strength of strengthening material. The maximum confining stress is up to 2.2 MPa, which significantly improves the compressive strength and the ultimate strain. The strength of core concrete is increased by 21–33% and the ultimate strain is enhanced to beyond 15,000 $\mu\varepsilon$.

Acknowledgements The tests reported herein were made possible by the financial support from National Natural Science Foundation of China (Grant Nos. 51708240 and 51678456).

References

Abdalla, S., Abed, F., & AlHamaydeh, M. (2013). Behavior of CFSTs and CCFSTs under quasi-static axial compression. *Journal of Constructional Steel Research, 90,* 235–244.

Abed, F., AlHamaydeh, M., & Abdalla, S. (2013). Experimental and numerical investigations of the compressive behavior of concrete filled steel tubes (CFSTs). *Journal of Constructional Steel Research, 80,* 429–439.

Abedi, K., Afshin, H., & Shirazi, M. R. N. (2010). Numerical study on the seismic retrofitting of reinforced concrete columns using rectified steel jackets. *Asian Journal of Civil Engineering, 11*(2), 219–240.

Aboutaha, R. S., Engelhardt, M. D., Jirsa, J. O., & Kreger, M. E. (1999a). Rehabilitation of shear critical concrete columns by use of rectangular steel jackets. *ACI Structural Journal, 96*(1), 68–78.

Aboutaha, R. S., Engelhardt, M. D., Jirsa, J. O., & Kreger, M. E. (1999b). Experimental investigation of seismic repair of lap splice failures in damaged concrete columns. *ACI Structural Journal, 96*(2), 297–306.

Aboutaha, R. S., & Machado, R. I. (1999). Seismic resistance of steel-tube high-strength reinforced-concrete columns. *Journal of Structural Engineering, 125*(5), 485–494.

Adam, J. M., Ivorra, S., Giménez, E., Moragues, J. J., Miguel, P., Miragall, C., et al. (2007). Behavior of axially loaded RC columns strengthened by steel angles and strips. *Steel and Composite Structures, 7*(5), 405–419.

Chen, W. F., & Saleeb, A. F. (1982). *Constitutive equation for engineering materials*. New York: Wiley.

Colomb, F., Tobbi, H., Ferrier, E., & Hamelin, P. (2008). Seismic retrofit of reinforced concrete short columns by CFRP materials. *Composite Structures, 82*(4), 475–487.

Dai, J. G., Bai, Y. L., & Teng, J. G. (2011). Behavior and modeling of concrete confined with FRP composites of large deformability. *Journal of Composites for Construction, 15*(6), 963–973.

Elremaily, A., & Azizinamini, A. (2002). Behavior and strength of circular concrete-filled tube columns. *Journal of Constructional Steel Research, 58*(12), 1567–1591.

Gupta, P. K., Sarda, S. M., & Kumar, M. S. (2007). Experimental and computational study of concrete filled steel tubular columns under axial loads. *Journal of Constructional Steel Research, 63*(2), 182–193.

Hadi, M. N. S. (2007). Behavior of FRP strengthened concrete columns under eccentric compression loading. *Composite Structures, 77*(1), 92–96.

Han, L. H., Li, W., & Bjorhovde, R. (2014). Developments and advanced applications of concrete-filled steel tubular (CFST) structures: Members. *Journal of Constructional Steel Research, 100,* 1186–1195.

Han, L. H., Liao, F. Y., Tao, Z., & Hong, Z. (2009). Performance of concrete filled steel tube reinforced concrete columns subjected to cyclic bending. *Journal of Constructional Steel Research, 65*(8–9), 1607–1616.

Han, L. H., & Yao, G. H. (2004). Experimental behaviour of thin-walled hollow structural steel (HSS) columns filled with self-consolidating concrete (SCC). *Thin-Walled Structures, 42*(9), 1357–1377.

Han, L. H., Yao, G. H., & Zhao, X. L. (2005). Tests and calculations for hollow structural steel (HSS) stub columns filled with self-consolidating concrete (SCC). *Journal of Constructional Steel Research, 61*(9), 1241–1269.

Han, L. H., Zheng, L. Q., He, S. H., & Tao, Z. (2011). Tests on curved concrete filled steel tubular members subjected to axial compression. *Journal of Constructional Steel Research, 67*(6), 965–976.

Holschemacher, K. (2004). Hardened material properties of self-compacting concrete. *Journal of Civil Engineering and Management, 10*(4), 261–266.

Julio, E. N. B. S., & Branco, F. A. B. (2008). Reinforced concrete jacketing-interface influence on cyclic loading response. *ACI Structural Journal, 105*(4), 471–477.

Kwan, A. K. H., Dong, C. X., & Ho, J. C. M. (2016). Axial and lateral stress-strain model for concrete-filled steel tubes. *Journal of Constructional Steel Research, 122,* 421–433.

Li, C. Q., & Melchers, R. E. (2005). Time-dependent risk assessment of structural deterioration caused by reinforcement corrosion. *ACI Structural Journal, 102*(5), 754–762.

Lu, F. W., Li, S. P., & Sun, G. J. (2007). A study on the behavior of eccentrically compressed square concrete-filled steel tube columns. *Journal of Constructional Steel Research, 63*(7), 941–948.

Lu, Y. Y., Liang, H. J., Li, S., & Li, N. (2015a). Eccentric strength and design of RC columns strengthened with SCC filled steel tubes. *Steel and Composite Structures, 18*(4), 833–852.

Lu, Y. Y., Liang, H. J., Li, S., & Li, N. (2015b). Axial behavior of RC columns strengthened with SCC filled square steel tubes. *Steel and Composite Structures, 18*(3), 623–639.

Miller E. A. (2006). *Experimental research of reinforced concrete column strengthening methods*. Master Thesis, The Ohio State University. pp. 24–30, 222–230.

Muciaccia, G., Giussani, F., Rosati, G., & Mola, F. (2011). Response of self-compacting concrete filled tubes under eccentric compression. *Journal of Constructional Steel Research, 67*(5), 904–916.

Parvin, A., & Wang, W. (2002). Concrete columns confined by fiber composite wraps under combined axial and cyclic lateral loads. *Composite Structures, 58*(4), 539–549.

Priestley, M. J. N., Seible, F., Xiao, Y., & Verma, R. (1994a). Steel jacket retrofitting of reinforced concrete bridge columns for enhanced shear strength-part 1: Theoretical considerations and test design. *ACI Structural Journal, 91*(4), 394–405.

Priestley, M. J. N., Seible, F., Xiao, Y., & Verma, R. (1994b). Steel jacket retrofitting of reinforced concrete bridge columns for enhanced shear strength-part 2: Test results and comparison with Theory. *ACI Structural Journal, 91*(5), 537–551.

Sakino, K., Nakahara, H., & Morino, S. (2004). Nishiyama, behavior of centrally loaded concrete-filled steel-tube short columns. *Journal of Structural Engineering ASCE, 130*(2), 180–188.

Sezen, H., & Miller, E. A. (2011). Experimental evaluation of axial behavior of strengthened circular reinforced-concrete columns. *Journal of Bridge Engineering, 16*(2), 238–247.

Tao, Z., Uy, B., Liao, F. Y., & Han, L. H. (2011). Nonlinear analysis of concrete-filled square stainless steel stub columns under axial compression. *Journal of Constructional Steel Research, 67*(11), 1719–1732.

Uy, B., Tao, Z., & Han, L. H. (2011). Behaviour of short and slender concrete-filled stainless steel tubular columns. *Journal of Constructional Steel Research, 67*(3), 360–378.

Vandoros, K. G., & Dritsos, S. E. (2008). Concrete jacket construction detail effectiveness when strengthening RC columns. *Construction and Building Materials, 22*(3), 264–276.

Wang, M. H. (2011). Experimental study on axial-compression reinforced concrete column strengthened by circular steel tube. *Applied Mechanics and Materials, 94,* 1261–1270.

Xiao, Q. G., Teng, J. G., & Yu, T. (2010). Behavior and modeling of confined high-strength concrete. *Journal of Composites for Construction, 14*(3), 249–259.

Xiao, Y., & Wu, H. (2003). Strengthening of reinforced concrete columns using partially stiffened steel jackets. *Journal of Structural Engineering, 129*(6), 725–732.

Yalcin, C., & Saatcioglu, M. (2000). Inelastic analysis of reinforced concrete columns. *Computers & Structures, 77*(5), 539–555.

Zhou, M., Li, J. W., & Duan, J. M. (2012). Experimental study on the axial loading tests of RC columns strengthened with steel tube. *Applied Mechanics and Materials, 204,* 2878–2882.